Tertiary Interactions with the Internal Guide Sequence Mediate Docking of the P1 Helix into the Catalytic Core of the *Tetrahymena* Ribozyme†

Scott A. Strobel and Thomas R. Cech*

Howard Hughes Medical Institute, Department of Chemistry and Biochemistry, University of Colorado, Boulder, Colorado 80309-0215

Received August 10, 1993®

ABSTRACT: The L-21 *Sca*I ribozyme catalyzes sequence-specific cleavage of an oligonucleotide substrate. Cleavage is preceded by base pairing of the substrate to the internal guide sequence (IGS) at the 5′ end of the ribozyme to form a short RNA duplex (P1). Tertiary interactions between P1 and the catalytic core dock P1 into the active site of the ribozyme. These include interactions between the catalytic core and 2′-hydroxyls of the substrate at nucleotide positions −3u and perhaps −2c. In this study, 2′-hydroxyls of the IGS strand that contribute to P1 recognition by the ribozyme are identified. IGS 2′-hydroxyls (nucleotide positions 22–27) were individually modified to either 2′-deoxy or 2′-methoxynucleotides within full-length semisynthetic L-21 *Sca*I ribozymes generated using T4 DNA ligase. Thermodynamic and kinetic characterization of the resulting IGS variant ribozymes justify the following conclusions: (i) 2′-Hydroxyls at nucleotide positions G22 and G25 play a critical energetic role in docking P1 into the catalytic core, contributing 2.6 and 2.1 kcal·mol^{-1}, respectively. (ii) The loss of binding energy is manifest primarily as an increase in the rate of dissociation. Because turnover for the wild-type ribozyme is limited by product dissociation, G22 and G25 deoxy variants display up to a 20-fold increase in the multiple-turnover rate at saturating substrate. (iii) IGS tertiary interactions are energetically coupled with the tertiary interactions made to the substrate, consistent with P1 becoming undocked from its binding site in J8/7 upon substitution of either the G22 or G25 2′-hydroxyl. (iv) The G22 deoxy variant loses energetic coupling between guanosine and substrate binding, suggesting that in this variant the P1 helix is also undocked from its binding site in J4/5, the proposed site of guanosine and substrate interaction. Therefore, in combinations with previous studies four P1 2′-hydroxyls are implicated as important for docking. The contributions of the 2′-hydroxyl tertiary interactions are not equivalent and follow the hierarchical order G22 > G25 ≫ −3u > −2c. Because the G22 2′-hydroxyl appears to mediate P1 docking into both J8/7 and J4/5, it may serve as the molecular linchpin for the recognition of P1 by the catalytic core.

The L-21 *Sca*I ribozyme form of the group I intron from *Tetrahymena thermophila* preribosomal RNA catalyzes sequence-specific cleavage of oligonucleotide substrates (S) (Zaug et al., 1986; 1988). Cleavage proceeds by a transesterification mechanism involving nucleophilic attack by the 3′-hydroxyl of guanosine (G) (reviewed in Cech et al., 1992). Substrate binds to the ribozyme by a two-step mechanism (Herschlag, 1992; Bevilacqua et al., 1992). First, the substrate binds by base pairing to a complementary internal guide sequence (IGS) at the 5′ end of the ribozyme to form a short RNA duplex called P1 (Figure 1) (Davies et al., 1982; Inoue et al., 1985b; Been & Cech, 1986; Waring et al., 1986). Second, P1 docks into the active site of the ribozyme by tertiary interactions between P1 and the RNA catalytic core (Pyle & Cech, 1991; Bevilacqua & Turner, 1991; Herschlag et al., 1993a).

The molecular basis of the interaction between the P1 duplex and the catalytic core of the ribozyme is only partially understood. Mutagenesis and phylogenetic comparisons of different group I introns demonstrated the requirement for a U·G pair at the cleavage site (Davies et al., 1982; Doudna et al., 1989a; Barfod & Cech, 1989; Michel & Westhof, 1990). At all other positions, base pairing within the helix rather than a particular sequence is required, suggestive that base-specific contacts do not play a prominent role in the molecular recognition of this RNA duplex by the ribozyme (Davies et al., 1982; Been & Cech, 1986; Waring et al., 1986; Murphy & Cech, 1989). However, tertiary interactions between the substrate strand of P1 and the ribozyme were implicated by the finding that oligoribonucleotides, but not oligodeoxyribonucleotides, bind to the ribozyme ≈ 4 kcal mol^{-1} stronger than expected for base-pairing alone (Sullivan & Cech, 1985; Sugimoto et al., 1988; Sugimoto et al., 1989a,b; Herschlag & Cech, 1990c; Pyle et al., 1990). The significance of this docking energy is exemplified by the ability of a ribozyme lacking an IGS to bind an exogenous P1 helix and use it as a reaction substrate (Doudna & Szostak, 1989b; Doudna et al., 1991).

The extra binding energy can be explained by sequence-nonspecific contacts to the RNA backbone. Two such interactions with the substrate strand of P1 have been proposed. 2′-Hydroxyls at base positions −2c and −3u (Figure 1)

† This work was supported by a Life Sciences Research Foundation fellowship sponsored by the Howard Hughes Medical Institute to S.A.S. T.R.C. is an Investigator of the Howard Hughes Medical Institute and an American Cancer Society Professor. We thank the W. M. Keck Foundation for support of RNA science on the Boulder campus.

* Author to whom correspondence should be addressed.

® Abstract published in *Advance ACS Abstracts*, November 15, 1993.

[1] Abbreviations: G, guanosine; pG, guanosine-5′-monophosphate; S, substrate [rGGCCCUCUAAAAA]; P, product of S cleavage[rGGCCCUCU]; d2P [rGGCCCUd(C)rU]; d3P [rGGCCCd(U)rCU]; dp [dGGCCCUCU]; E, L-21 *Sca*I ribozyme; IGS, internal guide sequence; P1, paired region 1 consisting of the IGS base paired to an oligonucleotide substrate or product; MES, 2-(*N*-morpholino)ethanesulfonic acid; tris, tris(hydroxylmethyl)aminomethane; PAGE, polyacrylamide gel electrophoresis; EDTA, (ethylenedinitrilo)tetraacetic acid; DMS, dimethyl sulfate.

0006-2960/93/0432-13593$04.00/0

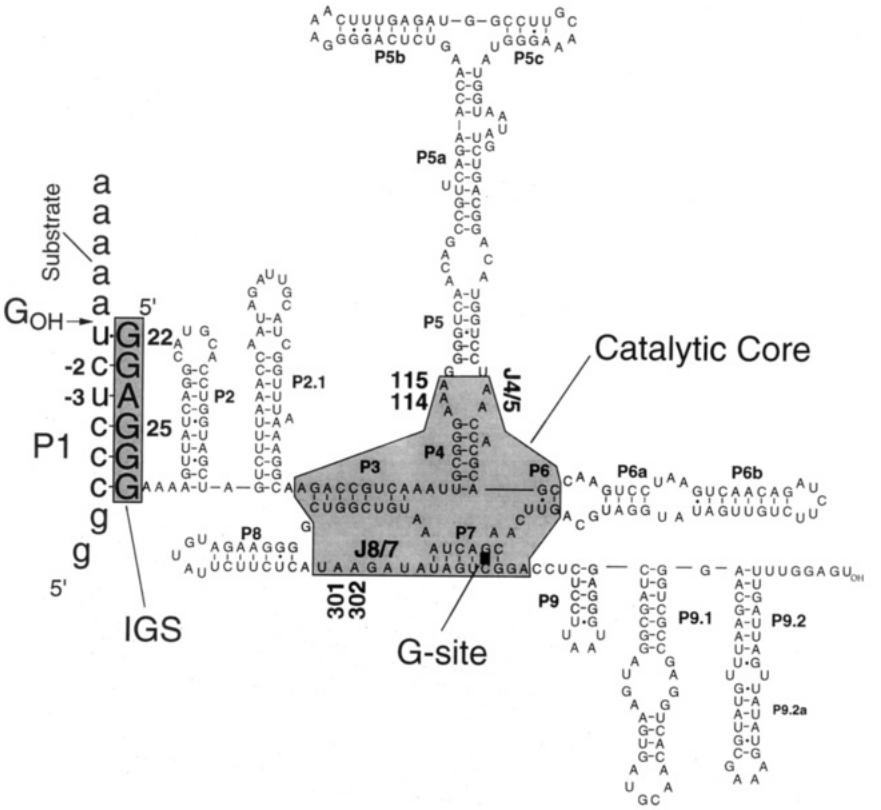

FIGURE 1: Primary and secondary structure of the L-21 *Sca*I ribozyme form of the *Tetrahymena* intron. The RNA substrate (lowercase letters) is shown bound to the internal guide sequence (IGS) (gray rectangle) forming the P1 helix. The phylogenetically conserved catalytic core of the ribozyme which includes the site of P1 docking and G binding is shown in gray. The nucleotides examined in this study are indicated by number corresponding to their base position in the full-length intron. The single-stranded joining regions J4/5 and J8/7 are also indicated. In this paper, J4/5 is used to refer to both strands of the internal loop joining P4 and P5.

contribute approximately 0.6 and 1.6 kcal·mol^{-1} of free energy to P1 docking, respectively, beyond that attributed to simple helix stabilization (see *wt* ribozyme, Table I). The tertiary interaction with –3u was mapped to a phylogenetically conserved adenine (A302) in the J8/7 region of the catalytic core. A specific hydrogen bond was postulated between the 2′-hydroxyl of –3u and the N1 of A302 (Pyle et al., 1992). No tertiary interaction with –2c has yet been identified.

The IGS strand of the P1 duplex might make additional tertiary contacts to the catalytic core via 2′-hydroxyls as postulated previously (Michel & Westhof, 1990; Pyle et al., 1992). The ability to make specific 2′-hydroxyl substitutions within large semisynthetic RNA molecules was recently demonstrated using T4 DNA ligase and a DNA splint (Moore & Sharp, 1992). To investigate the possible role of IGS 2′-hydroxyls in P1 docking, we individually modified each 2′-hydroxyl group of the IGS within full-length semisynthetic ribozymes and characterized them for their ability to bind and cleave oligonucleotide substrates. We find that interactions between the IGS and catalytic core are localized to two of the 2′-hydroxyl groups, each of which contributes significantly to P1 docking.

MATERIAL AND METHODS

Materials. Unlabeled nucleoside triphosphates were purchased from Pharmacia, [γ-^{32}P]ATP from New England Nuclear, guanosine-5′-monophosphate (pG) from Sigma, T4 polynucleotide kinase and *Sca*I endonuclease from New England Biolabs, DNA polymerase and dideoxynucleotides from U.S. Biochemical Corporation, and AMV reverse transcriptase from Life Sciences. T4 DNA ligase was a gift from U.S. Biochemical Corporation. T7 RNA polymerase was prepared from *Escherichia coli* strain BL21 containing the plasmid pAR1219 (Davanloo et al., 1984).

Oligonucleotide Preparation. RNA substrates (S) (G_2-CCCUCUA_5), products (P) (G_2CCCUCU), and IGS oligoribonucleotides (Figure 2) (including all chimeric RNA/DNA oligonucleotides) were prepared by solid-phase synthesis on an Applied Biosystems 380B DNA synthesizer using β-cyanoethyl phosphoramidite chemistry. Deprotection was completed in concentrated NH_4OH/ethanol (3:1) overnight at 55 °C, followed by removal of the silyl protecting groups with tetrabutylammonium fluoride in tetrahydrofuran overnight at room temperature. Oligoribonucleotides were desalted by passage through a NAP25 column (Pharmacia), dried by vacuum centrifugation, purified to nucleotide resolution by denaturing 15–20% PAGE, visualized by UV shadowing, and eluted in 10 mM Tris, 1 mM EDTA, 250 mM NaCl overnight. The oligonucleotides were desalted and concentrated using a Sep-Pak reverse phase disposable cartridge with elution in 40% acetonitrile in H_2O, dried, and stored at –20 °C until use. DNA oligomers were deprotected in concentrated NH_4OH at 55 °C overnight, dried, and purified to nucleotide resolution as described above. Oligonucleotide concentrations were determined by absorbance at 260 nm (Borer, 1975; Richards, 1975).

Oligonucleotide substrates and products were 5′-end-labeled using [γ-^{32}P]ATP and T4 polynucleotide kinase. The oligomers were purified by nondenaturing 20% PAGE, eluted into 300 μL of 10 mM tris (pH 7.5), 1 mM EDTA overnight at 4 °C, and used without additional precipitation. The concentration of the ^{32}P labeled oligonucleotides was estimated from the specific activity of the [γ-^{32}P]ATP and the labeled RNA.

Plasmid Construction. Plasmid pTZL-38HA was constructed from parent plasmid pTZL-21HA (Grosshans & Cech 1991) by oligonucleotide-directed phagemid mutagenesis (Kunkel et al., 1987). Plasmid pTZL-38HA contains a T7

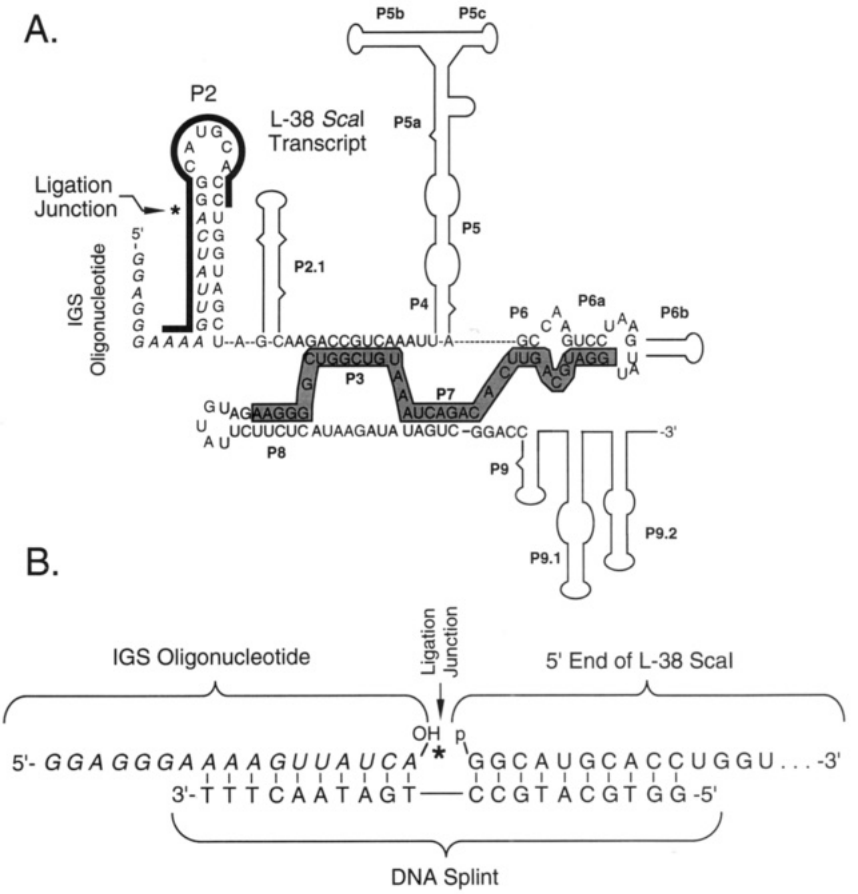

FIGURE 2: Schematic representation of the reaction components used to construct semisynthetic L-21 *Sca*I ribozymes by ligation. A. Components of the ligation reaction include a synthetic 17 base IGS oligonucleotide (italicized sequence), an L-38 *Sca*I transcript (sequence and helices) lacking the first 17 5′-terminal bases normally present in the L-21 *Sca*I transcript, a DNA splint (thick black line) complementary to the 3′ end of the IGS oligonucleotide and the 5′ end of the L-38 *Sca*I transcript, and a disrupter DNA oligonucleotide complementary to sequence (shaded box) in the structural core of the ribozyme. B. The ligation junction including a 3′-hydroxyl and a 5′-phosphate. The ligation junction is shown with the sequences of the IGS oligonucleotide (italics), the 5′ end of the L-38 *Sca*I transcript, and the DNA splint. Phosphodiester bond formation at the junction is catalyzed by T4 DNA ligase.

RNA polymerase promoter proximal to nucleotide position 38 of the intron and yields an RNA transcript 17 bases shorter at the 5′ end than the transcript from the parent plasmid. The site of transcription initiation was chosen within the P2 helix at the sequence GG to maximize transcription efficiency by T7 RNA polymerase (Milligan et al., 1987). The sequence of the ribozyme coding region of the plasmid was confirmed by dideoxy sequencing (Sanger et al., 1977).

Ribozyme Preparation. The L-21 *Sca*I wild-type (*wt*-all ribose) ribozyme was prepared by run-off transcription from *Sca*I-linearized pTZL-21HA plasmid DNA as described previously (Zaug et al., 1988).

Semisynthetic ribozymes containing single 2′-deoxy- or 2′-methoxynucleotide substitutions within the IGS were prepared by ligation of a synthetic 17-base IGS chimeric oligonucleotide to an L-38 RNA *Sca*I transcript by T4 DNA ligase using a DNA splint (Figure 2) (Moore & Sharp, 1992). L-38 *Sca*I RNA containing predominantly 5′ monophosphate was obtained by T7 RNA polymerase transcription using a GMP to GTP ratio of 10:1. Transcription conditions were 40 mM tris-HCl, pH 7.5, 12 mM $MgCl_2$, 1 mM each NTP, 10 mM GMP, 10 mM dithiothreitol, 4 mM spermidine, 0.05% Triton X-100, 20 μg/mL *Sca*I-linearized pTZL-38HA DNA, and 5000 units/mL T7 RNA polymerase at 37 °C for 1 h. Transcripts were purified by denaturing 4% PAGE, visualized briefly by UV shadowing, eluted from the gel as described above for oligonucleotides, and precipitated with three volumes of ethanol.

The L-38 *Sca*I RNA transcript was hybridized to the IGS oligonucleotide in two steps. First, the transcript was annealed to a disrupter oligonucleotide complementary to much of the sequence in the catalytic core (Figure 2A). Excess disrupter oligonucleotide (5.0 nmol) was added to 2.5 nmol L-38 *Sca*I RNA in 250 μL 10 mM tris-HCl, pH 7.5 and 1 mM EDTA, heated to 90 °C, and cooled to 35 °C over 15 min. In a separate reaction the 17 base RNA IGS oligonucleotide (5.0 nmol) was annealed to 5 nmol of a 20 base DNA splint complementary to the 3′ end of the IGS oligonucleotide and the 5′ end of the L-38 transcript using identical buffer conditions in 150 μL at 23 °C. In the second step of annealing, the two solutions were combined and splint/IGS oligonucleotide complex annealed to the L-38 transcript at 23 °C for 30 min (Figure 2B). Following hybridization, ligation buffer and T4 DNA ligase were added to bring the solution to 67 mM tris-HCl, pH 7.8, 6.7 mM $MgCl_2$, 10 mM DTT, 0.5 mM ATP, and 100 units DNA ligase/nmol transcript (250 units) in a final volume of 500 μL and allowed to react for 6–8 h at 23 °C. Ligated products were separated from starting material by denaturing 4% PAGE and recovered from the gel as described above.

The integrity of the ligation junction in all variants was confirmed by run-off primer extension using reverse transcriptase (Zaug et al., 1984). Complete primer extension was observed for the majority of the isolated ribozymes (90% as quantitated by PhosphorImager analysis), a level slightly below that measured for a ribozyme made entirely by transcription. Most ribozymes had a small amount (typically 5%) of termination at a size consistent with L-38 unligated material. This remained after gel purification due to the difficulty of separating molecules 371 and 388 nucleotides in

length on a large scale. Because the L-38 lacks the IGS and is incompetent to bind substrate, a simple correction was made to the ribozyme concentrations measured by absorbance at 260 nm ($\epsilon_{260} = 3.2 \times 10^6$ M^{-1} cm^{-1})(Zaug et al., 1988). The ribozymes were further characterized by dideoxy chain termination sequencing to confirm the sequence at the ligation junction and by alkaline hydrolysis to confirm the location of the 2′-deoxy- or 2′-methoxynucleotide substitutions. For the ribozymes that displayed the most dramatic effects the chimeric oligonucleotides were resynthesized, the ribozymes religated, and the new ribozymes characterized to the extent necessary to confirm the validity of the results.

Dissociation Constants. Equilibrium dissociation constants (K_d, K_d^C, and K_{rel}) for the binding of P [$rG_2CCCUCU$], d2P [$rG_2CCCUd(C)rU$], and d3P [$rG_2CCCd(U)rCU$] were measured in 10 mM $MgCl_2$, 50 mM tris pH 7.5, 0.1 mM EDTA, 10 mM NaCl, 3% glycerol, 0.05% xylene cyanol at 42 °C (Pyle et al., 1990). Binding of dP [$dG_2CCCUCU$] was measured at 25 °C. Ribozymes were preincubated with buffer for 20 min at 50 °C to insure conformational homogeneity and then incubated with oligonucleotide(s) for 10–120 min to insure equilibrium binding. All variant ribozymes showed identical results for both incubation periods indicating they had reached equilibrium after 10 min. The *wt* and *wt** ribozymes had a lower K_d and required approximately 60 min to reach equilibrium (Pyle et al., 1992). The bound and unbound fractions were separated under native gel conditions (10 mM $MgCl_2$, 33 mM tris pH 7.5, 66 mM HEPES, and 0.1 mM EDTA) using a 10% polyacrylamide gel with 29:1 cross-linking ratio. The fraction of product bound was quantitated by PhosphorImager analysis (Molecular Dynamics).

Direct Band Shift. Equilibrium dissociation constants for product binding (K_d^P) by each of the ribozymes were determined by the band shift method using 0.01 nM radiolabeled *P* (*P**) such that $[P^*] \ll K_d^P$. The fraction of *P** bound (θ) was measured as a function of total ribozyme concentration (*E*) and fit to the equation

$$\theta = \frac{E}{E + K_d^P} \quad (1)$$

Competition Band Shift. Equilibrium dissociation constants for P, d2P, d3P, and dP binding were determined by competition band shift (Weeks & Crothers, 1992). A ribozyme concentration equal to approximately twice the K_d^P for each variant (70% bound in the absence of competitor) was combined with a trace amount (0.01 nM) of *P** and 0.035 nM to 100 μM unlabeled competitor. The fraction of *P** bound (θ) decreased as the competitor concentration increased. θ was used to calculate the competitor dissociation constant (K_d^C) by solving the quadratic expression (Lin & Riggs, 1972)

$$\theta = \frac{1}{2P^*}\left\{K_d^P + \frac{K_d^P \cdot C}{K_d^C} + E + P^* - \left[\left(K_d^P + \frac{K_d^P \cdot C}{K_d^C} + E + P^*\right)^2 - 4P^*E\right]^{1/2}\right\} \quad (2)$$

using a nonlinear least-squares routine where *E*, *P**, and *C* are the concentrations of ribozyme, radiolabeled *P**, and competitor oligonucleotide, respectively, and K_d^P is the dissociation constant for *P** as measured above. K_d^C for P, d2P, and d3P were determined for *wt* and each of the variant ribozymes. Relative dissociation constants (K_{rel}) for d2P and d3P were calculated for each ribozyme as a ratio to K_d^C for *P*.

Kinetics. General methods followed those previously described (Herschlag & Cech, 1990a,b; Herschlag et al., 1991). Measurements of k_c and K_d^G were performed as per McConnell et al. (1993). Unless otherwise indicated, reactions were performed in 10 mM $MgCl_2$, 50 mM MES, pH 7.0, at 30 °C. As these conditions are different from those used for the band shift assay, all conclusions are made relative to *wt**. Ribozymes were preincubated in reaction buffer for 20 min at 50 °C to produce conformational homogeneity prior to cooling the ribozyme to 30 °C and initiating the reaction by the addition of substrate and guanosine. Portions of the reaction were removed at various times and quenched on ice with two volumes 7.5 M urea, 20 mM EDTA, 0.1% xylene cyanol, and 0.1% bromophenol blue. Reaction products were resolved from substrate by denaturing 20% PAGE and the fraction reacted quantitated by PhosphorImager analysis. Unless otherwise indicated kinetic determinations were made under single-turnover conditions, ribozyme concentration in excess, and the reactions followed for three half-lives. All reactions obeyed first-order kinetics, with an end-point of 10–15% unreactive substrate. Reactions performed at 50 °C showed only 5% unreactive material as previously observed (Herschlag & Cech, 1990a). The specific reaction conditions utilized for each experiment are described in the figure legends.

RESULTS

Construction of Semisynthetic Ribozymes by Ligation. T4 DNA ligase catalyzes the formation of a phosphodiester linkage between a 3′-hydroxyl and a 5′-monophosphate juxtaposed within double-stranded nucleic acid (Lehman, 1974; Moore & Sharp, 1992). For ligation of the semisynthetic L-21 *Sca*I ribozyme, these requirements were met in the following way (Figure 2): (i) Synthesis and deprotection of the 17-base IGS oligonucleotide yielded a 3′-hydroxyl without additional modification. (ii) A 5′-monophosphate was incorporated into approximately 90% of the L-38 *Sca*I transcripts by initiating transcription with a GMP to GTP ratio of 10:1. (iii) A DNA oligonucleotide splint with ten base complementarity to each RNA was used to juxtapose the ligation substrates. Additionally, hybridization of a disrupter oligonucleotide complementary to sequence throughout the structural core improved the ligation efficiency and made the reaction significantly less sensitive to the buffer conditions of splint hybridization. The disrupter persumably prevents tertiary structure formation of the L-38 *Sca*I transcript making the 5′ end more accessible to split hybridization. Ligation efficiencies of 75–80% were achieved after 8 h with little product degradation using 100 units ligase/nmol transcript. Longer incubation times resulted in slightly higher efficiencies, but lower absolute yields due to gradual degradation of the RNA. The ribozyme yield after all steps was 10–20% of the initial L-38 *Sca*I RNA.

For this study ten ribozymes were constructed by ligation. The first ribozyme, designated *wt**, has an IGS composed entirely of ribose nucleotides. Six of the ribozymes contain single 2′-deoxyribose substitutions at each of the six nucleotide positions within the IGS, bases 22–27 of the intron (Figure 1). The final three ribozymes contain single 2′-methoxy substitutions at base positions 22, 23, and 25. The ligated ribozymes are designated in italics by the type of chemical substitution followed by the base position of the change, i.e., *d22* contains a 2′-deoxy-guanosine at position 22, *OMe23* contains a 2′-methoxyguanosine at position 23, etc. Ribozyme *wt** serves as the standard of comparison for ribozymes containing backbone substitutions in the IGS. It is also used to compare the activities of a semisynthetic and a fully

Table I: Equilibrium Dissociation Constants and Free Energies for Modification of 2′-Hydroxyls on the P and IGS Strands of the P1 Helix

ribozyme	oligomer	K_d^P[a] (nM)	K_{rel}[b]	$\Delta\Delta G°_{obs}$[c] (kcal·mol^{-1})	$\Delta\Delta G°_{tertiary}$[d] (kcal·mol^{-1})
wt	P	0.3 ± 0.1[e]	(1)	(0)	
	d1P	0.8 ± 0.2[f]	2.7	0.6	0.0
	d2P	1.9 ± 0.4[f]	6.3	**1.2**	**0.6**
	d3P	10 ± 2[f]	33	**2.2**	**1.6**
	d4P	0.9 ± 0.2[f]	3.0	0.7	0.1
	d5P	0.8 ± 0.2[f]	2.7	0.6	0.0
*wt**	P	0.35 ± 0.1	(1)	(0)	
d22	P	130 ± 30	370	**3.7**	**2.6**
d23	P	4.2 ± 1.7	12	1.6	0.5
d24	P	0.8 ± 0.2	2.3	0.5	−0.6
d25	P	60 ± 20	170	**3.2**	**2.1**
d26	P	5.3 ± 1.0	15	1.7	0.6
d27	P	1.4 ± 0.2	4.0	0.9	−0.2
OMe22	P	130 ± 20	370	**3.7**	
OMe23	P	0.2 ± 0.1	0.7	−0.2	
OMe25	P	180 ± 30	510	**4.0**	

[a] Reported values are the average of at least two exponential trials. [b] K_{rel} for the substrate strand is calculated as a ratio of the *wt* K_d for P, d1P, d2P, d3P, d4P, or d5P to the K_d for P, e.g., $K_{rel}^{d3P} = K_d^{d3P}/K_d^P$. By definition K_{rel}^P is 1. K_{rel} for the IGS strand is calculated as a ratio of K_d^P of each variant to the K_d^P of *wt**, e.g., $K_{rel}^P(d22) = K_d^P(d22)/K_d^P$ (*wt**). By definition K_{rel}^P(*wt**) is 1. [c] $\Delta\Delta G°_{obs}$ is equal to $-RT \ln (1/K_{rel})$ where T is 315 K and R is 0.001 98 kcal·mol^{-1}·K^{-1}. This value represents the total destabilization (duplex and tertiary) resulting from 2′-deoxy substitution at each position in the substrate strand. Values in parentheses are zero by definition. $\Delta\Delta G°_{obs}$ values that are significantly above the background level for duplex destabilization on each strand are shown in bold letters. [d] $\Delta\Delta G°_{tertiary}$ values are calculated by subtracting the energy attributable to duplex destabilization (0.6 kcal·mol^{-1} for the substrate strand and 1.1 kcal·mol^{-1} for the IGS strand; see text) from the total energetic destabilization of the substitution. These values are interpreted to be the tertiary interaction energy for each 2′-hydroxyl. Values that are significantly above background are indicated in bold. [e] This value was originally reported as 0.8 nM (Pyle & Cech, 1991) but later corrected to 0.3 nM (Pyle et al., 1992). K_{rel} and $\Delta\Delta G°_{obs}$ for the substrate strand are recalculated using the corrected value. [f] As reported in Table I of Pyle and Cech (1991).

transcribed ribozyme (*wt*). Although *wt* and *wt** are identical in sequence and both exclusively contain ribose sugars, *wt* has a terminal 5′-triphosphate whereas *wt** and all the semisynthetic ribozymes terminate in a 5′-hydroxyl.

Hydroxyls at Positions 22 and 25 Are Critical for P1 Docking. The equilibrium dissociation constant for P binding (K_d^P) for each of the ribozymes was measured (Figure 3). The results are summarized in Table I. Ribozyme *wt** has the same K_d^P as *wt*. This confirms that an all-ribose semisynthetic ribozyme lacking the terminal 5′-triphosphate is fully competent for binding. Ribozyme *wt** is also equivalent to *wt* for all other thermodynamic and kinetic assays performed in this study.

All of the deoxy-substituted ribozymes bind P less tightly than *wt** (Table I). These variants are categorized into two subgroups based upon the magnitude of K_d^P and whether the binding energy can be rescued by introduction of a 2′-methoxy substitution.

Two of the ribozymes, *d22* and *d25*, bind P substantially weaker than *wt** or the other deoxy variants (Table I). Deoxy substitution at G22 and G25 have 400- and 200-fold effects on K_d^P, representing a loss of 3.7 and 3.2 kcal·mol^{-1}, respectively. This is at least 2 kcal·mol^{-1} more destabilizing than observed with the other variants. Approximately 1.1 kcal·mol^{-1} of the free energy can be assigned to duplex destabilization due to deoxy substitution (see below). We assign the remaining free energy, 2.6 and 2.1 kcal·mol^{-1} for G22 and G25 2′-hydroxyls, respectively, to loss of tertiary interactions with the catalytic core.

The assignment of this free energy to docking is supported by 2′-methoxy substitutions at G22 and G25. 2′-Deoxynucleotides favor the C2′ endo conformation while 2′-hydroxy- and 2′-methoxynucleotides favor the C3′ endo sugar conformation (Uesugi et al., 1979; Guschlbauer & Jankowski, 1980; Chou et al., 1989; Katahira et al., 1990; Salazar et al., 1993; Jaishree et al., 1993). A 2′-methoxy substitution eliminates the 2′-position as a hydrogen bond donor and provides some steric bulk that may preclude it as a hydrogen bond acceptor. However, it reestablishes duplex stability (Herschlag et al., 1993a), presumably because it restores the C3′ endo sugar pucker found in A-form duplex RNA. Despite these compensating effects on duplex stability, 2′-methoxy substitutions at G22 and G25 fail to restore binding. K_d^P of *OMe22* and *d22* are identical, and *OMe25* binds P almost 3-fold weaker than *d25*. In contrast, 2′-methoxy substitution at G23 restores binding (see below). Therefore, although 2′-methoxy substitutions restore duplex stability, an additional contribution to binding is not recovered with 2′-methoxy substitutions at nucleotide positions G22 and G25. This reinforces the conclusion that these two 2′-hydroxyls are involved in tertiary interactions with the catalytic core. Additionally, the lack of restoration by methoxy substitution suggests that both of these hydroxyls serve as hydrogen bond donors.

The K_d^P values for the second subgroup of ribozymes, *d23*, *d24*, *d26*, and *d27*, range from 1 to 5 nM, indicating a 1.1 ± 0.6 kcal·mol^{-1} average loss of oligonucleotide binding energy at each position compared to *wt**. Based on the arguments discussed below, we assign the 2–10-fold K_d^P effect observed for the second subgroup of IGS backbone variants to duplex destabilization resulting from the altered sugar pucker of the deoxy substitution in an otherwise all-RNA duplex.

The assignment of 1.1 kcal·mol^{-1} to duplex destabilization on the substrate strand of P1 rather than tertiary hydrogen bonding contacts at these four positions is supported by 2′-methoxy substitution at position 23. The K_d^P of *OMe23* is 0.2 nM, slightly more stable than *wt** (0.35 nM), and substantially more stable than *d23* (4.2 nM). This is consistent with restoration of duplex stability by reestablishment of the proper sugar pucker. A similar stabilizing effect was observed with methoxy substitutions at noncritical positions on the product half of the helix (Herschlag et al., 1993a). Because *d23* has one of the highest K_d^P's among the second subclass of ribozymes, the methoxy result argues against the involvement of G23, A24, G26, and G27 2′-hydroxyls in tertiary contacts with the catalytic core of the ribozyme, and supports the use of data from this subgroup as a measure of helix destabilization.

Although 1.1 kcal·mol^{-1} is approximately 0.5 kcal·mol^{-1} more destabilizing than the average deoxy substitution within the product half of the duplex (0.6–0.7 kcal·mol^{-1} from Pyle & Cech, 1990; 0.4–0.9 kcal·mol^{-1} from Bevilacqua & Turner, 1991), the difference is likely due to the sequence composition of the two strands. The substrate strand of P1 is composed exclusively of pyrimidines and the IGS strand exclusively of purines. Measurements of the thermodynamic stability of polynucleotide and model RNA:DNA hybrid duplexes has consistently demonstrated that binding of a purine-rich DNA strand to a pyrimidine-rich RNA strand (purDNA:pyrRNA) is less stable than either a purRNA:pyrRNA or a purRNA:pyrDNA duplex (Chamberlin & Patterson, 1965; Riley et al., 1966; Martin & Tinoco, 1980; Walker, 1988; Hall & McLaughlin, 1991). This is postulated to result from enthalpic stabilization of the purRNA strand resulting from greater intrastrand stacking when the purine strand is in the A-conformation (Walker, 1988; Hall & McLaughlin, 1991).

Table II: Equilibrium Dissociation Constants and Free Energies for Simultaneous Modification of 2′-Hydroxyls on the S and IGS Strands of the P1 Helix

ribo-zyme	compe-titor	K_d^C[a] (nM)	K_{rel}[b]	$\Delta\Delta G°_{obs}$[c] (kcal mol^{-1})	$\Delta\Delta G°_{tertiary}$[d] (kcal mol^{-1})
wt	P	0.1 ± 0.0	(1)	(0)	
	d2P	0.8 ± 0.1	7.5 ± 1.3	1.3	0.4
	d3P	6.4 ± 0.5	58 ± 12	2.5	1.6
*wt**	P	0.2 ± 0.0	(1)	(0)	
	d2P	2.8 ± 0.3	14 ± 2	1.6	0.7
	d3P	13 ± 2	72 ± 20	2.7	1.8
d22	P	190 ± 30	(1)	(0)	
	d2P	620 ± 40	3.6 ± 1.0	0.8	**–0.1**
	d3P	490 ± 40	2.9 ± 0.7	0.7	**–0.2**
d23	P	3.9 ± 0.8	(1)	(0)	
	d2P	47 ± 4	12 ± 2	1.5	0.6
	d3P	170 ± 30	45 ± 4	2.4	1.5
d24	P	0.7 ± 0.1	(1)	(0)	
	d2P	9.4 ± 1.3	14 ± 2	1.6	0.7
	d3P	48 ± 13	68 ± 18	2.6	1.7
d25	P	44 ± 3	(1)	(0)	
	d2P	170 ± 20	3.7 ± 0.6	0.8	**–0.1**
	d3P	290 ± 50	6.7 ± 1.2	1.2	**0.3**
d26	P	5.0 ± 1.3	(1)	(0)	
	d2P	55 ± 10	11 ± 1	1.5	0.6
	d3P	160 ± 30	34 ± 8	2.2	1.3
d27	P	1.3 ± 0.2	(1)	(0)	
	d2P	13 ± 3	10 ± 2	1.4	0.5
	d3P	93 ± 6	61 ± 8	2.6	1.7

[a] All values for K_d^C were independently determined for each ribozyme by competition gel shift with P, d2P, or d3P as competitor (Figure 4). The values represent the average of at least two experimental trials. For each ribozyme the values for K_d^C with P as competitor are in good agreement with the K_d^P values reported in Table I. Additionally, the K_d^C values for *wt* binding to d2P and d3P are in good agreement with the K_d values measured by direct band shift (Table I). [b] K_{rel} is calculated as a ratio of K_d^C for P, d2P, or d3P to the K_d^C for P for each ribozyme, e.g., $K_{rel}^{d2P}(d22) = K_d^{C(d2P)}(d22)/K_d^{C(P)}(d22)$. By definition K_{rel}^P is 1 for each ribozyme. [c] $\Delta\Delta G°_{obs}$ is equal to $-RT \ln (1/K_{rel})$ where T is 315 K and R is 0.001 98 kcal·mol^{-1}·K^{-1}. This value represents the total destabilization (duplex and tertiary) resulting from 2′-deoxy substitution at –2c or –3u. [d] $\Delta\Delta G°_{tertiary}$ is equal to $\Delta\Delta G°_{obs}$ minus 0.9 kcal·mol^{-1} attributable to duplex destabilization from a 2′-deoxy substitution on the substrate strand of P1 as measured in this assay. $\Delta\Delta G°_{tertiary}$ represents the destabilization of P1 docking caused by a 2′-deoxy substitution at –2c or –3u.

Modification of the Critical 2′-Hydroxyls on the IGS Strand Disrupts Tertiary Interactions with the Substrate Strand. Substitutions on the substrate strand of P1 revealed two independent tertiary interactions involving 2′-hydroxyls at –2c and –3u, contributing approximately 0.6 and 1.6 kcal·mol^{-1} to P1 docking, respectively (Pyle & Cech, 1991) (Table I). The 2′-hydroxyls at G22 and G25 each contribute more than 2 kcal·mol^{-1} to P1 docking (Table I). This is more than usually observed for the loss of a single hydrogen bond (Turner et al., 1987; Santa Lucia et al., 1991, 1992). The difference might be accounted for in many ways, but one intriguing possibility is that the magnitude of the docking free energy for *d22* and *d25* results from concomitant loss of tertiary interactions on both strands of P1 upon modification of the critical IGS 2′-hydroxyls. If the IGS and substrate strand tertiary interactions are energetically coupled, i.e., cooperative, then modification of the G22 or G25 2′-hydroxyls will attenuate the docking energy derived from the –2c and –3u 2′-hydroxyls. Chimeric oligonucleotide products d2P [rG$_2$CCCUd(C)rU] and d3P [rG$_2$CCCd(U)rCU] each lack one of the substrate strand 2′-hydroxyls implicated in tertiary interactions with the core. If the substrate strand interactions are unaffected when P is bound to *d22* or *d25*, then d2P and d3P should bind approximately 1.5 and 2.5 kcal·mol^{-1} weaker than P (see *wt* and *wt** in Table II). At the other extreme, if the IGS modifications eliminate the substrate strand tertiary interactions, then the 2′-deoxynucleotide substitutions in d2P and d3P should affect binding only to the extent of duplex destabilization (≈0.5–1.0 kcal·mol^{-1}).

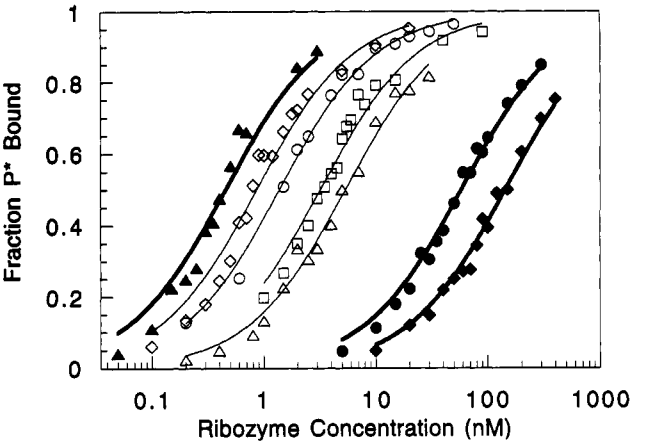

FIGURE 3: Oligonucleotide binding by the ribozyme is affected by 2′-deoxy substitutions in the IGS. Semilog plots of fraction 5′-^{32}P labeled G$_2$CCCUCU (P*) bound versus ribozyme concentration for *wt** (▲), *d22* (◆), *d23* (□), *d24* (◇), *d25* (●), *d26* (○), and *d27* (△) as measured by band shift. Each line represents fit of data to eq 1.

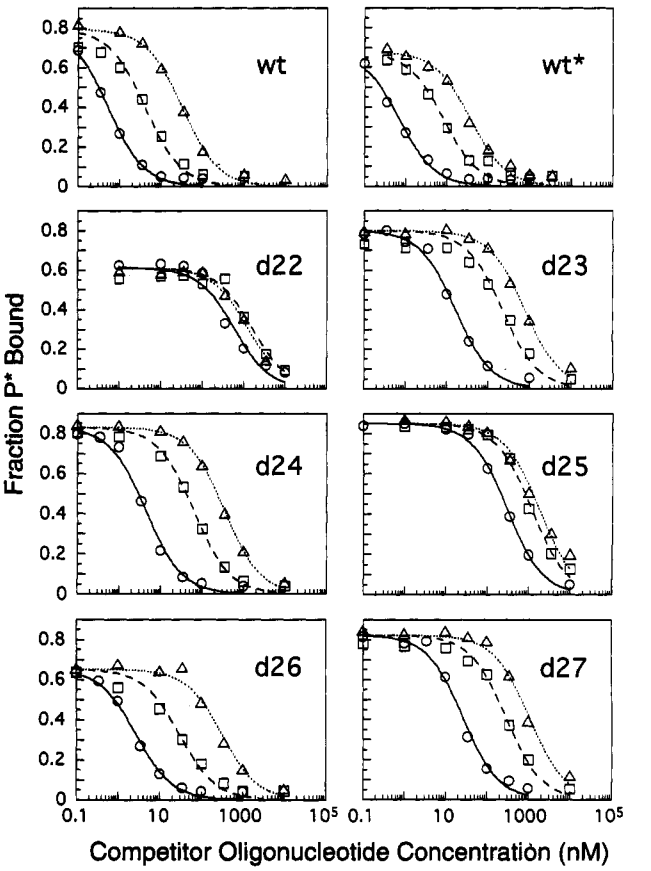

FIGURE 4: Energetic coupling of 2′-hydroxyl interactions on the substrate and IGS strands determined by competition. Semilog plots of fraction 5′-^{32}P labeled rG$_2$CCCUCU (P*) bound versus concentration of oligonucleotide competitor for P (○), d2P [rG$_2$CCCUd(C)rU] (□), and d3P [rG$_2$CCCd(U)rCU] (△). The ribozyme concentration is approximately 2-fold above K_d^P resulting in 70–80% of P* bound in the absence of competitor. Each line represents fit of data to eq 2.

To determine how disruption of the IGS tertiary interactions affects interactions with the substrate strand, we measured the equilibrium dissociation constants (K_d^C) of P, d2P, and d3P for each of the 2′-deoxy variant ribozymes by competitive band shift (Figure 4). The results are presented in Table II. Assuming the energetic contributions of the –2c and –3u 2′-hydroxyls of P remain approximately 0.6 and 1.6 kcal·mol^{-1}

Table III: Equilibrium Dissociation Constants of dP ($dG_2CCCUCU$) Binding at 25 °C[a]

ribozyme	K_d^{Pb} (nM)	K_d^{dPb} (nM)	K_{rel}[c]	$\Delta\Delta G°_{obs}$[d] (kcal mol^{-1})	$\Delta\Delta G°_{tertiary}$[e] (kcal mol^{-1})
wt		200 ± 30	(1)	(0)	
d22	4.3	15000 ± 10000	75	2.5	**2.1**
d23	0.04	450 ± 200	2.2	0.5	0.1
d25	0.8	5000 ± 3000	25	1.9	**1.5**
d27	0.05	330 ± 100	1.7	0.3	−0.1

[a] Experiments were performed at 25 °C to reduce the K_d^{dP} for the variant ribozymes into a range that could be experimentally determined. [b] The K_d^{dP} values are the average of at least two trials. The K_d^{dP}(*wt*) was measured by band shift with ^{32}P-5′-end-labeled dP (0.15 nM). For the variant ribozymes the K_d^{dP} was measured by competition band shift with 0.005 nM ^{32}P-5′-end-labeled P (P*) and unlabeled dP competitor. Ribozymes were incubated at 25 °C with P* and dP for 3 h to establish equilibrium. Ribozyme concentrations were *d22* 10 nM; *d23* 0.4 nM; *d25* 5 nM; and *d27* 0.4 nM. dP concentrations ranged from 32 nM to 100 μM. To solve for the K_d^{dP} by competition gel shift from eq 2, the K_d^{P} must also be known at 25 °C. This was determined for each of the variant ribozymes by direct band shift using a 3-h incubation of 0.005 nM P* with ribozyme. [c] K_{rel} is the ratio of the K_d^{dP} of the variant ribozymes to the K_d^{dP}(*wt*), e.g., K_{rel}(*d22*) = K_d^{dP}(*d22*)/K_d^{dP}(*wt*). By definition K_{rel}(*wt*) is 1. [d] $\Delta\Delta G°_{obs}$ is equal to $-RT$ ln $(1/K_{rel})$ where T is 298 K and R is 0.001 98 kcal·mol^{-1}·K^{-1}. This value represents the total destabilization (duplex and tertiary destabilization) resulting from 2′-deoxy substitutions in the IGS when it is bound to an all-deoxynucleotide product. [e] $\Delta\Delta G°_{tertiary}$ is equal to $\Delta\Delta G°_{obs}$ minus 0.4 kcal·mol^{-1} duplex destabilization determined by measurement of the *d23* and *d27* ribozymes. $-\Delta\Delta G°_{tertiary}$ represents the tertiary binding energy contributed by 2′-hydroxyls within the IGS when bound to an all-deoxynucleoside product.

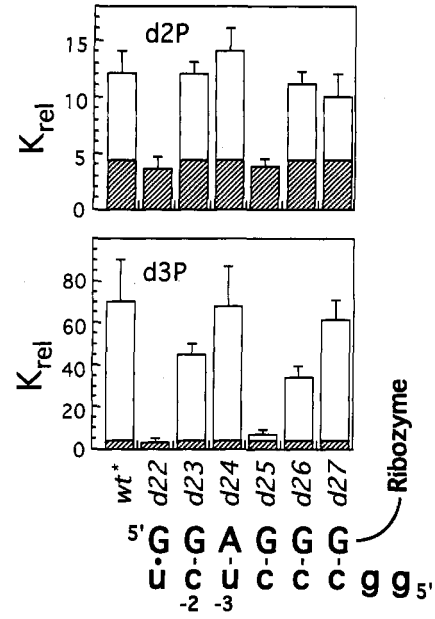

FIGURE 5: Relative dissociation constants (K_{rel}) of *wt* and semisynthetic ribozymes for chimeric oligonucleotide products d2P [rG_2-CCCUd(C)rU] and d3P [rG_2CCCd(U)rCU]. Each constant is expressed relative to binding of P [rG_2CCCUCU] by the same ribozyme; e.g., K_{rel}(d2P) = K_d^{d2P}/K_d^{P}. The scales for d2P and d3P are different reflecting the observation that the 2′-hydroxyl at −3u makes a larger contribution to docking than the 2′-hydroxyl at −2c. The darkened area in each bar represents the average extent of duplex destabilization (approximately 4-fold) expected for substituting a single deoxynucleotide on the substrate strand of the P1 helix. The white area in each bar corresponds to destabilization attributable to loss of tertiary interaction between P1 and the catalytic core. The sequence of the P1 helix with IGS bound to P is shown below the bar graphs.

for the *wt* and *wt** ribozymes, then the background duplex destabilization measured by this assay (≈0.9 kcal·mol^{-1}) appears to be slightly higher than that measured by direct band shift (≈0.6 kcal·mol^{-1}) (Pyle & Cech, 1990). All of the variant ribozymes bind d2P and d3P weaker than P, however not to an equal extent. For ribozymes *d22* and *d25* the free energy difference between binding of P and binding of either chimeric oligonucleotide ($\Delta\Delta G°_{obs}$) ranges from 0.7–1.2 kcal·mol^{-1}. If helix destabilization is subtracted from $\Delta\Delta G°_{obs}$, little or no energy remains that can be attributed to tertiary interactions (Figure 5). However, noncritical variants *d23*, *d24*, *d26*, and *d27* have $\Delta\Delta G°_{obs}$ values that are essentially equal to that of *wt**, approximately 1.5 and 2.5 kcal·mol^{-1} for d2P and d3P binding, respectively. When helix destabilization is subtracted from $\Delta\Delta G°_{obs}$ for these variants, approximately 0.6 and 1.6 kcal·mol^{-1} remains that can be attributed to tertiary interactions for −2c and −3u, respectively (Table II). These data are consistent with the hypothesis that modification of critical tertiary interactions on the IGS strand disrupts interactions with the substrate strand.

Modification of Critical 2′-Hydroxyls on the Substrate Strand Does Not Disrupt IGS Strand Tertiary Interactions. Because modification of the IGS tertiary interactions results in the concomitant attenuation of the substrate strand contacts, we wished to determine the effect of substrate strand 2′-hydroxy modification upon the IGS tertiary interactions. We measured the K_d for binding of a deoxynucleotide product, dP ($dG_2CCCUCU$), in which all of the substrate strand 2′-hydroxyls are missing. All four of the variant ribozymes tested bind dP less tightly than does *wt* (Table III). However, ribozymes *d22* and *d25* bind dP 2.1 and 1.5 kcal·mol^{-1} weaker, respectively, than *d23* and *d27*, two ribozymes used as controls to approximate the extent of duplex destabilization due to introduction of a single deoxynucleotide in the RNA strand of this DNA:RNA hybrid. Thus, to a large extent the tertiary contacts to the IGS are maintained even when the ribozyme is bound to an all-deoxy product. Consistent with this conclusion, a ribozyme derivatized at G22 with an azidophenacyl moiety undergoes photocross-linking to J4/5 when bound to either an all-ribose (P) or an all-deoxyribose product (dP) (Wang et al., 1993).

The data from Table III also argue against an alternative model in which there are no interactions between 2′ hydroxyls at G22 and G25 and the core. In this model 2′-deoxy or methoxy substitutions at these two positions somehow prevent P1 docking, and the energetic destabilization observed for *d22* and *d25* binding to P simply results from the loss of interactions with the substrate strand at positions −2c and −3u. If this were the case, then *d22*, *d23*, *d25*, and *d27* would bind dP, which cannot derive any stabilization from substrate strand 2′-hydroxyl groups, with approximately equal affinity. In contrast to this expectation, *d22* and *d25* bind dP more weakly than do *d23* and *d27* (Table III). Therefore, it appears that 2′-hydroxyls at G22 and G25 make a direct positive contribution to binding and indirectly facilitate contributions by 2′-hydroxyls at −2c and −3u of the substrate strand.

Attempts to directly assess the thermodynamic relationship between the two critical IGS 2′-hydroxyls by making the doubly substituted ribozyme were unsuccessful. The K_d^{P} for *d22* is 130 nM at 42 °C. Substitution of a second 2′-deoxy nucleotide results in the loss of an additional kcal·mol^{-1} solely due to duplex destabilization. This results in a theoretical K_d^{P} of more than 1 μM which is much greater than can be measured by the band shift assay. Additionally, the amount of ribozyme needed to perform such an experiment is prohibitive. Therefore, the relationship between the G22 and G25 2′-hydroxyls and the individual enzymatic rate constants were assayed by kinetics.

Overview of Ribozyme Kinetics. The kinetic pathway of the ribozyme reaction has been extensively characterized and is summarized for the *wt* ribozyme in Figure 6 (Herschlag &

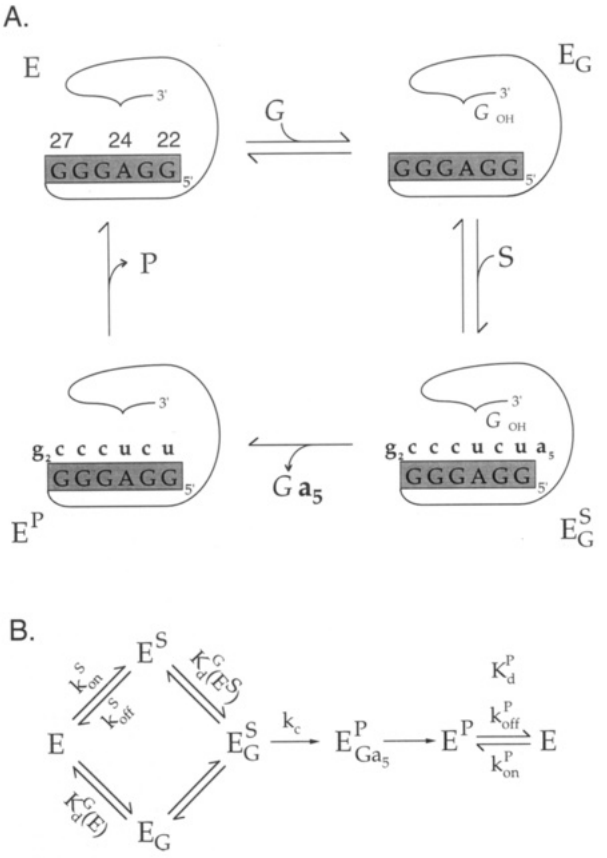

FIGURE 6: Cleavage of oligonucleotide substrate by the *wt* ribozyme. A. The cycle of ribozyme-catalyzed cleavage of S. The IGS is shown in a gray box. The ribozyme complexes are shown schematically: E, free ribozyme; E_G, ribozyme with guanosine bound at the G binding site; E^S, ribozyme with substrate bound to the IGS (not shown); E^S_G, ribozyme with G and S bound; and E^P, ribozyme with oligonucleotide product bound to the IGS. B. Kinetic scheme adopted from Herschlag and Cech (1990a) showing the individual rate and dissociation constants of interest in this study. S and G bind the ribozyme in either order. Modest coupling is observed between G and S binding in the *wt* ribozyme such that the K^G_d for a ribozyme with bound substrate (E^S) is not equal to the K^G_d for a ribozyme free of substrate (E) (McConnell et al., 1993). The resulting ternary complex reacts rapidly with the rate constant k_c to produce two products. GA_5 is released very quickly from the ribozyme. The $G_2CCCUCU$ product is released slowly such that for the *wt* ribozyme under k_{cat} conditions k^P_{off} is rate-limiting (Herschlag & Cech, 1990a).

Cech, 1990a–c; Herschlag et al., 1991; Young et al., 1991). The reaction catalyzed by the ribozyme (E) involves two substrates: guanosine (G) and an oligonucleotide (S) partially complementary to the IGS. The ribozyme binds G and S in either order with modest energetic coupling between the binding of these two substrates (McConnell et al., 1993; Bevilacqua et al., 1993). The E^S_G complex goes through a chemical transition involving nucleophilic attack by the 3′-hydroxyl of G on the substrate to form two oligonucleotide products. The first oligomer (GA_5), which has the G nucleophile jointed to its 5′ end, rapidly dissociates from the ribozyme. The second product (P; $G_2CCCUCU$) is bound to the ribozyme by base pairing with the IGS and tertiary contacts between P1 and the catalytic core. P slowly dissociates from the IGS, which regenerates the ribozyme in its initial form. Under the appropriate concentrations of E, S, and G, individual rate constants in the reaction pathway can be monitored.

The Substrate Association Rate Is Unaffected by IGS Modifications. The K^P_d measured by band shift reflects the ratio of product dissociation (k^P_{off}) and association (k^P_{on}) rate constants. To identify the kinetic parameters responsible for the observed increase in K^P_d the rate of S association (k^S_{on}) was measured utilizing the kinetics of S cleavage. The second-order rate constant $(k_{cat}/K_m)^S$ can be measured under single-turnover conditions (E in excess of S) by varying the ribozyme concentration under conditions of low E and saturating G. $(k_{cat}/K_m)^S$ is the rate constant for reaction of E_G (guanosine fully bound to the ribozyme but the substrate binding site unoccupied) and free S. For the *wt* ribozyme the rate-limiting step under these conditions is substrate binding, such that $(k_{cat}/K_m)^S$ is equal to k^S_{on} (Herschlag & Cech, 1990a). k^S_{on} and k^P_{on} each measure the rate of helix formation and are equal within a factor of 2–3 for *wt* and a series of variant ribozymes (Young et al., 1991).

Table IV: Kinetic Characterization of *wt*, *wt**, and 2′-Deoxynucleotide Substituted Ribozymes

ribozyme	$(k_{cat}/K_m)^S$ [a] (10^8 M^{-1} min^{-1})	k_{cat} [b] (min^{-1})	$(k_{cat}/K_m)^G$ [c] (10^5 M^{-1} min^{-1})
wt	1.1 ± 0.3	0.3 ± 0.1	2.4 ± 0.3
*wt**	1.0 ± 0.2	0.5 ± 0.2	2.1 ± 0.3
d22	0.7 ± 0.2	**20 ± 3**	**0.20 ± 0.03**
d23	0.8 ± 0.3	3 ± 1	2.2 ± 0.2
d24	1.1 ± 0.5	0.6 ± 0.3	2.8 ± 0.4
d25	0.3 ± 0.1	**9 ± 3**	1.4 ± 0.2
d26	0.7 ± 0.1	3 ± 0.2	1.9 ± 0.2
d27	0.6 ± 0.1	3 ± 1	1.8 ± 0.3

[a] From single-turnover reactions at 30 °C, 10 mM $MgCl_2$, 50 mM MES, pH 7.0 with 1.0 mM G, 0.5 nM 5′-^{32}P labeled S, and 2.5–20 nM ribozyme. [b] From multiple-turnover reactions performed at 50 °C in 50 mM MES pH 7.0 with 0.5 mM GMP, 10 mM $MgCl_2$, trace amount of ^{32}P labeled S, 2.5–10 nM ribozyme, and cold S at concentrations saturating for each ribozyme. S concentrations of 250–2000 nM were used for *wt*, *wt**, *d23*, *d24*, *d26*, and *d27*, and 2000–16 000 nM S for ribozymes *d22* and *d25*. Initial reaction rates were determined using data for cleavage of the first 25–30% of S. The large ratio of S to E prevented the accurate observation of an initial reaction burst, though the data were fit to include a burst of a size commensurate with the ribozyme concentration. [c] See legend to Figure 7.

Values of $(k_{cat}/K_m)^S$ for each of the deoxy-substituted ribozymes are presented in Table IV. None of the substitutions has a significant effect (greater than 3-fold) on $(k_{cat}/K_m)^S$, consistent with it being equal to k^S_{on} for these variants. The values k^S_{on} for all of the ribozymes are consistent with rate-limiting helix formation ($\approx 10^8$ M^{-1} min^{-1}). This indicates that the deoxy substitutions do not alter the accessibility of the IGS for P1 helix formation and implies that the increase in K^P_d is due to an increase in k^P_{off}.

The Increase in K^P_d Is Caused by an Increase in k^P_{off}. The first-order rate constant k_{cat} can be measured under multiple-turnover conditions (S in excess of E) with saturating S and saturating G. For *wt* k_{cat} is equal to the rate constant for P dissociation, k^P_{off}, a rate-limiting step that occurs after the chemical transition (Herschlag & Cech, 1990a). Therefore any increase in k_{cat} must mean an increase in k^P_{off}.

As predicted by the larger values of K^P_d, all of the ribozymes have faster multiple-turnover rates than *wt** (Table IV). This confirms that the increase in K^P_d is caused by an increase in the product dissociation rate (k^P_{off}). Additionally, the two ribozymes with the fastest multiple-turnover rates are *d22* and *d25*, proceeding 40- and 20-fold faster than *wt** ribozyme, respectively. The other ribozymes react only 2–6 fold faster than *wt**. The values for k_{cat} are in qualitative agreement with the higher values of K^P_d observed in the band shift experiments, although k_{cat} probably is not equal to k^P_{off} for all of the ribozymes.

Examination of G-Binding and the Chemical Step. The integrity of the catalytic center and the binding of G were examined by measuring $(k_{cat}/K_m)^G$ (Figure 7). Under single-

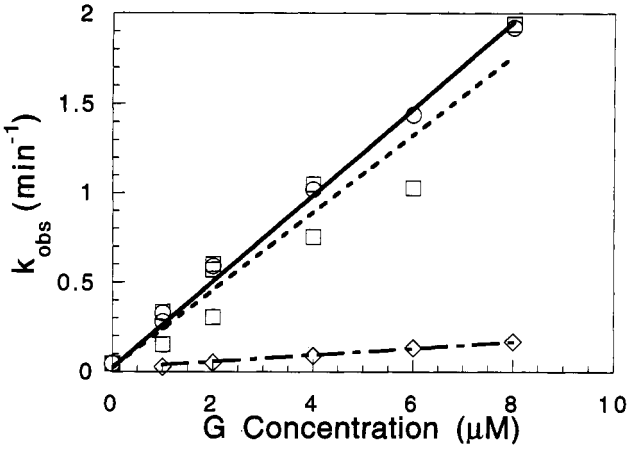

FIGURE 7: Measurement of the rate constant of the chemical step for the cleavage of S at pH 7.0 under conditions of saturating ribozyme for *wt* (○), *wt** (□), and *d22* (◇). Curve fits are linear with a Y intercept equal to the rate of hydrolysis for each ribozyme. $(k_{cat}/K_m)^G$ is equal to the slope. Data for *d23*, *d24*, *d26*, and *d27* are not shown but are similar to *wt**. Reactions were single turnover at 30 °C, 10 mM $MgCl_2$, 50 mM MES, pH 7.0, 0.5 nM 5′-^{32}P labeled S, 0–8 μM G and saturating ribozyme. 100 nM ribozyme was used for *wt*, *wt**, *d23*, *d24*, *d26*, and *d27*, and 500 nM for *d22* and *d25*. Concentrations were doubled in all cases with no significant change in rate to insure the ribozyme was at saturation.

turnover conditions $(k_{cat}/K_m)^G$ represents the second-order rate constant for the reaction of E^S (substrate fully bound to the ribozyme but the G binding site unoccupied) with free G. For the *wt* ribozyme $(k_{cat}/K_m)^G$ is limited by the chemical transition (Herschlag et al., 1991, 1993b).

All variant ribozymes have the same $(k_{cat}/K_m)^G$ as *wt** except *d22* which is 10-fold slower (Table IV). The *d22* $(k_{cat}/K_m)^G$ effect might reflect a change in the rate of the chemical transition or in the binding affinity of the ribozyme for G. It is interesting that despite *d22* and *d25* having very similar values for K_d^P, only *d22* is slow for $(k_{cat}/K_m)^G$. This implies that although similar in some ways, the removal of the 2′-hydroxyls at G22 and G25 are not equivalent. Investigation of the cause of the 10-fold reduction in $(k_{cat}/K_m)^G$ for *d22* revealed an important difference between ribozymes *d22* and *d25*.

Ribozyme d22 Is Defective in G-Binding. Reduction of the reaction pH from 7.0 to 5.5 facilitates the deconvolution of the two parameters that might cause the reduction in $(k_{cat}/K_m)^G$ for *d22*. The pH reduction slows the maximal rate of chemistry (k_c) from approximately 20 min^{-1} to less than 1 min^{-1} at 30 °C. Additionally, at pH 5.5 under single-turnover conditions the K_m^G is equal to K_d^G, and k_{cat} is equal to k_c, the rate constant for the actual chemical step (McConnell et al., 1993). Thus, both potential causes of the *d22* $(k_{cat}/K_m)^G$ effect can be directly measured.

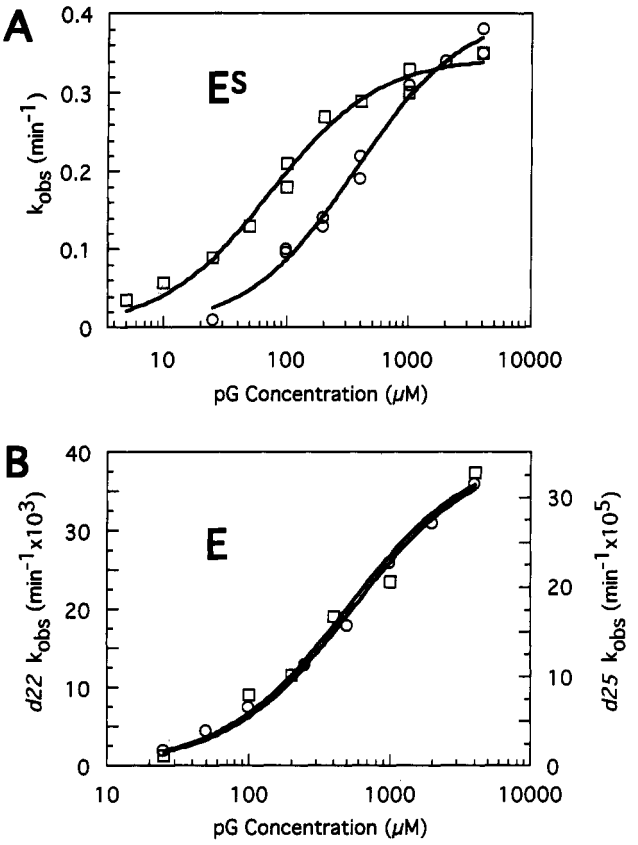

FIGURE 8: Measurement of $K_d^G(E^S)$, $K_d^G(E)$, and the rate constant for chemistry (k_c). A. Reactions of E^S at varying pG concentrations for *d22* (○) and *d25* (□) were performed at 30 °C in 10 mM $MgCl_2$, 50 mM MES pH 5.5 and with 0.5 nM ^{32}P-5′ end labeled S. pG concentrations were varied from 5–4000 μM using a saturating concentration of ribozyme: *d22*, 500 nM; *d25*, 300 nM. Each line represents the best nonlinear least squares fit of the data to the equation $k_{obs} = k_c[G]/\{K_d^G(E^S) + [G]\}$ solving for k_c and $K_d^G(E^S)$ (McConnell et al., 1993). B. Reactions of free E at varying pG concentrations for *d22* (○) and *d25* (□) were performed at 30 °C in 10 mM $MgCl_2$, 50 mM MES pH 5.5, and pG concentrations ranging from 50–4000 μM. For ribozymes *wt* (not shown) and *d25*, $K_d^G(E)$ was measured using 0.2 nM of ^{32}P-5′-end labeled dSr-1 [dCCCUCr(U)dA$_5$] and subsaturating ribozyme concentrations of 20 nM (*wt*) and 200 nM (*d25*). The K_d of dSr-1 is 2 μM and >10 μM for *wt* and *d25* ribozymes, respectively, at 42 °C (Pyle & Cech 1991; S. Strobel and T. Cech, unpublished results). Extremely slow cleavage was observed with *d22* using dSr-1 making accurate measurement of the cleavage rates difficult. To alleviate this problem the *d22* measurement of K_d^G for free E was made using d3S [rG$_2$CCCd(U)rCUA$_5$]. The K_d of *d22* for d3S at 42 °C is approximately 500 nM (Table II). 10 nM *d22* ribozyme was used as a subsaturating concentration. For both ribozymes data were fit to the equation $k_{obs} = (k_{cat}/K_m)^S[G]/\{K_d^G(E) + [G]\}$ by nonlinear least squares to solve for $K_d^G(E)$ (McConnell et al., 1993).

As reported in Table V, k_c remains unaffected for both variant ribozymes, but *d22* binds G 5-fold more weakly than *wt* or *d25* (Figure 8). This indicates that the *d22* $(k_{cat}/K_m)^G$ effect is not caused by a reduced rate of chemistry, but rather is due to a reduced affinity for G in the case of the *d22* E^S complex.[2]

Ribozyme d22 Has Lost Coupling between G and S Binding. The K_d^G is influenced by the substrate occupation state of the ribozyme (McConnell et al., 1993; Bevilacqua et al., 1993). McConnell et al. (1993) observed that the K_d^G for pG rose from 90 μM in the presence of substrate (E^S) to 360 μM in the absence of substrate (free E). This 1.0 kcal·mol^{-1} of coupling energy between G and S is lost if the P1 helix forms

[2] In light of the significant destabilization of P1 docking, it is surprising that neither ribozyme appears to have a reduced rate in the chemical step. Although the cause is not known, a reasonable hypothesis is as follows: Although the binding equilibrium has been shifted toward an undocked complex, P1 remains docked a sufficient fraction of the time for the apparent rate of chemistry to be unaffected. The apparent rate of chemistry in this system is modeled by the equation, $k_c = (k_2k_3)/(k_2 + k_{-2} + k_3)$, where k_2 and k_{-2} are the first-order rate constants for P1 docking and undocking, respectively, and k_3 is the rate constant for the actual chemical step (Bevilacqua et al., 1992). For the *wt* ribozyme, k_2 is greater than the sum of k_{-2} and k_3, and the equation is reduced to $k_c = k_3$ (Bevilacqua et al., 1992; McConnell et al., 1993). The fact that k_c for *d22* and *d25* is equal to k_c for *wt* suggests that, although the docking equilibrium is shifted toward an undocked conformation for both mutants, the denominator of the equation remains dominated by k_2 and, further, that K_2, the equilibrium constant for docking ($K_2 = k_2/k_{-2}$), remains greater than 1. Some docking in the absence of these important 2′-hydroxyl interactions implies that there are additional, as yet unidentified, contributions to P1 docking.

Table V: The Apparent Rate Constant for the Chemical Step at pH 5.5 and the Equilibrium Binding Constants of G for Ribozyme Bound to Substrate (E_S) and Free Ribozyme (E)

ribozyme	k_c[a] (min^{-1})	$K_d^G(E^S)$[a] (μM)	$K_d^G(E)$[a] (μM)
wt	0.40 ± 0.01	90 ± 7	330 ± 60
d22	0.41 ± 0.01	**360 ± 30**	**540 ± 50**
d25	0.36 ± 0.01	70 ± 8	500 ± 110

[a] See legend to Figure 8 for experimental conditions.

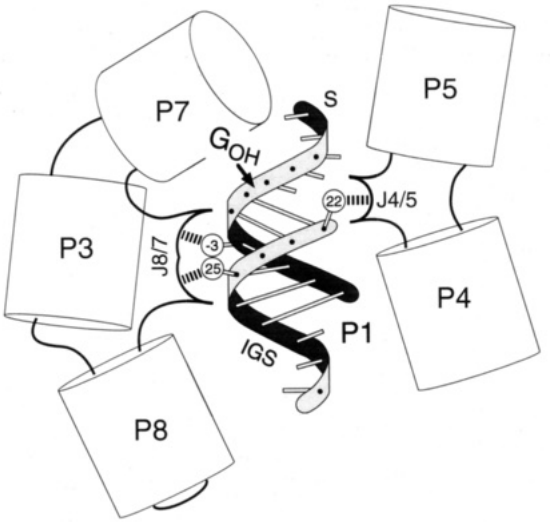

FIGURE 9: Model of the P1 helix docked into the catalytic core. Helices P3, P4, P5, P7, and P8 are shown as cylinders arranged according to the model of Michel and Westhof (1990). G is shown bound to the G binding site located in P7 (Michel et al., 1989). The single stranded joining regions J8/7 and J4/5 are depicted as black lines with the hydrogen bonding pockets for the docking of P1 drawn as semicircles. The P1 helix is shown as helical ribbons. The six bases of the IGS and the three bases of joining region J1/2 are shown bound to an 11 base oligonucleotide substrate (lacking the two 5′ terminal G's). Three of the 2′-hydroxyls critical for P1 docking are shown as large circles in the minor groove. The –2c 2′-hydroxyl is not shown, and the location of its interaction within the core is unknown. The hydrogen bonds postulated to occur between these hydroxyls and the catalytic core are depicted as heavy dashed lines.

but remains undocked from the catalytic center; and anti-cooperativity is observed between G and P. These data imply that the interaction occurs when the P1 helix is brought into proximity with the G nucleophile and is in some way mediated by the reactive phosphate or the adjacent A residue (McConnell et al., 1993; Bevilacqua et al., 1993). $K_d^G(E^S)$ for *d22* is in the range expected for loss of coupling between G and S, while $K_d^G(E^S)$ for *d25* is consistent with retention of coupling. $K_d^G(E)$ was measured to determine if the higher $K_d^G(E^S)$ for *d22* resulting from uncoupling of G and S.

Ribozymes *wt* and *d25* show the expected 5-fold coupling between G and S binding, but *d22* shows very little difference between G binding in the presence or absence of S (Figure 8 and Table V). The observation that *d22* has lost this coupling, while *d25* has retained it, suggests that the 2′-hydroxyl of G22 has a unique role among the 2′-hydroxyls of P1 in bringing the substrate into proximity with G, and therefore in docking P1 into the catalytic center.

Interaction Partners Remain Unidentified. Efforts were undertaken to identify the bonding partners for the two critical IGS 2′-hydroxyls. G22 forms a phylogenetically conserved wobble pair with the –1u located immediately 5′ to the cleavage site. G22 has been modeled to be proximal to the J4/5 region of the core with its 2′-hydroxyl hydrogen bonded to N1 of A114 (Michel & Westhof, 1990). Ribozymes derivatized at the G22 5′-hydroxyl with an azidophenacyl moiety show a strong photocross-link to A114/A115 in support of an assignment to this region (Wang et al., 1993). While the tentative assignment of the 2′-hydroxyl as a hydrogen bond donor is consistent with this model, DMS footprinting in the presence of saturating P showed no protection of the N1 at either of these bases in the presence or absence of the G22 hydroxyl (data not shown). Thus, although the model in combination with experimental data suggest that the G22 2′-hydroxyl interacts with the J4/5 loop, its specific bonding partner remains unidentified.

G25 forms a base pair with –4c. Based on the structure of an RNA helix, its 2′-hydroxyl must be juxtaposed with the 2′-hydroxyl of –3u in the minor groove of the P1 duplex. The –3u hydroxyl was shown to be important for P1 docking and based on mutagenesis and DMS footprinting it was postulated to interact with N1 of A302 (Pyle et al., 1992). These two structural constraints led to the proposal that the 2′-hydroxyl of G25 interacts with N1 of A301 (Pyle et al., 1992). The tentative assignment of the G25 2′-hydroxyl as a hydrogen bond donor is consistent with this proposal. The hypothesis was tested by DMS footprinting, however, and no selective reactivity at A301 was observed for the *d25* ribozyme (data not shown). It is still possible that N1 of A301 is the hydrogen bond acceptor, but deletion of the G25 2′-hydroxyl is insufficient to accommodate DMS. Thus, the bonding partner for G25 2′-hydroxyl remains unidentified, though the J8/7 single stranded region of the ribozyme remains an attractive candidate.

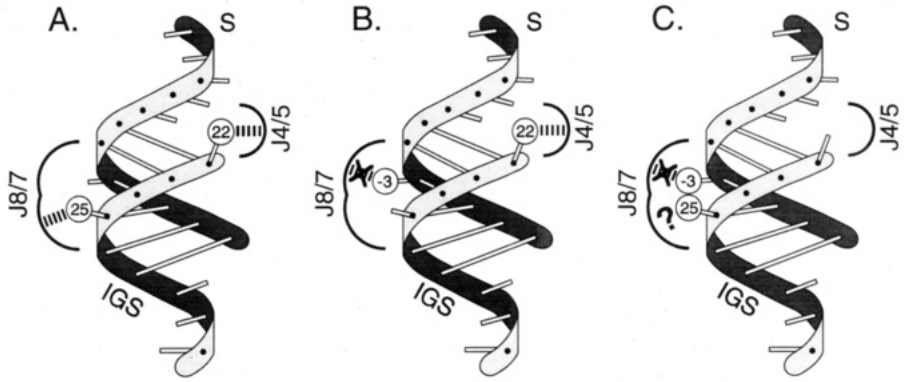

FIGURE 10: Hierarchy of tertiary contacts between P1 and the catalytic core. A. 2′-Deoxy substitution at –3u. B. 2′-Deoxy substitution at G25. C. 2′-Deoxy substitution at G22. See legend to Figure 9 for explanation of figure symbols. Only the joining regions J4/5 and J8/7 from the core are shown with each P1 helix. Deletion of a 2′-hydroxyl is depicted by removal of the circle representing the 2′-hydroxyl. Partial or complete loss of a hydrogen bond is represented with an X through the dashed line of the hydrogen bond. If the persistence of the hydrogen bond in unknown, the dashed line is replaced by a question mark.

DISCUSSION

Ribozymes Constructed by Ligation Are Fully Active. Full-length semisynthetic L-21 *Sca*I ribozymes were successfully constructed by ligation of a synthetic oligonucleotide to an RNA transcript using a DNA splint and T4 DNA ligase (Moore & Sharp, 1992). The all-ribose semisynthetic ribozyme and the fully transcribed ribozyme are identical for all kinetic and thermodynamic constants measured within the limits of experimental error. This is a powerful demonstration of the utility of ligation for generating large, fully active RNA molecules. Ribozymes containing single 2′-deoxy or 2′-methoxy substitutions at discrete positions within the IGS were constructed for this study. This represents the deletion of one atom (16 Daltons) at a specific position within an RNA molecule that contains more than 10 000 atoms and has a molecular weight over 100 000 Daltons.

A Model for P1 Docking into the Catalytic Core. Kinetic and thermodynamic characterization of the IGS variants demonstrate that the 2′-hydroxyls at positions G22 and G25 are critical for docking P1 into the catalytic center. The importance of being ribose at each position of the IGS decreases in the order 22G > 25G ≫ 23G, 26G, 27G > 24A. Mutation of the G22 or G25 2′-hydroxyls results in a significant increase in K_d^P, primarily due to an increase in k_{off}^P. 2′-Methoxy substitutions suggest that both hydroxyls serve as hydrogen bond donors, though steric hindrance by the bulky 2′-methoxyl group could also contribute to the failure of this derivative to compensate for binding. The data support the involvement of these 2′-hydroxyls in interactions with the catalytic core by either direct hydrogen bonding or through intermediary Mg^{2+} or water molecules. Although the bonding partners remain unidentified, model building combined with photocross-linking and affinity cleaving data place the G22 hydroxyl proximal to the J4/5 region which in turn is near the G nucleophile (Michel & Westhof, 1990; Wang & Cech, 1992; Wang et al., 1993). Model building using the –3u interaction with J8/7 as a constraint places the G25 hydroxyl proximal to J8/7 (Pyle et al., 1992). A model for the recognition of the P1 helix by the catalytic center that incorporates these new data with previous models of oligonucleotide recognition by the ribozyme is depicted in Figure 9.

While every potential hydrogen bonding atom within the P1 helix has not been specifically tested, a pattern of P1 recognition is beginning to emerge. P1 recognition involves interactions between 2′-hydroxyls lining the minor groove and functional groups in single-stranded regions or internal loops of the core. All of the proposed interactions are with functional groups of the backbone which are independent of the P1 sequence. It is likely the two interactions proposed in this study do not complete the list of P1 tertiary contacts. The ribozyme also appears to recognize some aspect of the U·G wobble (Doudna et al., 1989a; Barfod & Cech, 1989; Piccirilli et al., 1992; T. Chapman, A. M. Pyle, S. Moran, D. Turner, S. A. S., & T. R. C., unpublished results).

The Hierarchical Order of Tertiary Interactions. Four 2′-hydroxyls have now been proposed as important for P1 docking, though the effects of each hydroxyl are not equivalent. Based upon the thermodynamic effect of each 2′-hydroxyl modification and its relationship to the other interactions, the critical 2′-hydroxyls within P1 follow the hierarchical order G22 > G25 ≫ –3u > –2c. This ranking is supported by the following arguments. 2′-Hydroxyl contacts on the substrate strand of P1 at positions –2c and –3u make energetic contributions of approximately 0.6 and 1.6 kcal·mol^{-1}, respectively. The interactions are thermodynamically independent, i.e., the removal of one substrate-strand 2′-hydroxyl has little or no effect on other 2′-hydroxyl tertiary interactions made between the core and either strand of P1. 2′-Hydroxyl contacts on the IGS make a larger contribution to P1 docking, providing approximately 2.6 and 2.1 kcal·mol^{-1} at G22 and G25, respectively. Contributing to these large energetic effects is the concomitant disruption of both 2′-hydroxyl interactions on the substrate strand of P1 upon modification of either IGS 2′-hydroxyl. This suggests that proper alignment of both IGS tertiary interactions is necessary to dock P1 into J8/7, and only when the IGS is properly aligned will the core make thermodynamically significant tertiary interactions with the substrate strand. However, the energetic profiles of P1 docking upon modification of the G22 and G25 2′-hydroxyls are not equivalent. Energetic coupling between G and S binding is retained upon modification of G25, while the interaction is lost upon modification of G22. Affinity cleaving with an Fe(II)-EDTA derivative of G has shown that G is proximal to the J4/5 region of the ribozyme (Wang & Cech, 1992), and photocross-linking has shown that P1 is also near J4/5 (Wang et al., 1993). Together these data suggest that the 2′-hydroxyl of G22 has a unique role in bringing P1 into proximity with G, possibly in the J4/5 region of the ribozyme.

Model of P1 Docking with the Catalytic Core As a Function of 2′-Hydroxyl Modification. A model for P1 docking with the catalytic core upon mutation of critical P1 2′-hydroxyls is proposed in Figure 10.

P1 remains docked into J8/7 and J4/5 upon substitution of the critical substrate-strand 2′-hydroxyls (Figure 10A), but it is energetically destabilized. For example, 2′-deoxy substitution at position –3u destabilizes docking to an extent consistent with loss of one hydrogen bond to J8/7. However, modification at –3u does not significantly affect the energetic contribution of other P1 2′-hydroxyls interactions, i.e., G22 remains proximal to J4/5 and G25 to J8/7. A similar result is observed with –2c (not shown) though it makes less of an energetic contribution, and its binding partner in the core is unknown.

Substitution of the 2′-hydroxyl at G25 disrupts P1 docking into J8/7, but docking into J4/5 is unaffected (Figure 10B). Modification of the 2′-hydroxyl at G25 destabilizes P1 docking to an extent greater than typically observed for the loss of one hydrogen bond. This is the result of concomitant loss of the –2c and –3u tertiary interactions on the substrate strand and is consistent with partial or complete undocking of P1 from J8/7. However, the energetic coupling between G and S that occurs near the J4/5 region is unaffected, consistent with retention of the interaction between the G22 2′-hydroxyl and J4/5.

Finally, substitution of the 2′-hydroxyl at G22 disrupts the interaction energy to both J8/7 and J4/5 (Figure 10C). Like G25, modification of the G22 hydroxyl also results in the concomitant disruption of the –2c and –3u tertiary interactions. Loss of the –3u contact suggests that J8/7 is undocked in the G22 variant, though the effect of the G22 2′-hydroxyl upon that at G25 is not known (indicated by a question mark in Figure 10C). Additionally, energetic coupling of G and S is lost for the G22 variant consistent with undocking from J4/5. Because the G22 2′-hydroxyl appears to mediate P1 docking into both J8/7 and J4/5, it may serve as the molecular linchpin for the recognition of P1 by the catalytic core.

ACKNOWLEDGMENT

We thank A. Gooding and C. Grosshans for oligonucleotide synthesis and K. Weeks, T. McConnell, P. Bevilacqua, and D. Herschlag for helpful discussion of the experimental results.

REFERENCES

Barfod, E. T., & Cech, T. R. (1989) *Mol. Cell. Biol. 9*, 3657–3666.

Been, M. D., & Cech, T. R. (1986) *Cell 50*, 207–216.

Bevilacqua, P. C., & Turner, D. H. (1991) *Biochemistry 30*, 10632–10640.

Bevilacqua, P. C., Kierzek, R., Johnson, K. A., & Turner, D. H. (1992) *Science 258*, 1355–1358.

Bevilacqua, P. C., Johnson, K. A., & Turner, D. H. (1993) *Proc. Natl. Acad. Sci. U.S.A. 90*, 8357–8361.

Borer, P. N. (1975) in *Handbook of Biochemistry and Molecular Biology*: *Nucleic Acids* (Fasman, G. D., Ed.) 3rd ed., Vol. I, p 597, CRC Press, Cleveland, OH.

Cech, T. R., Herschlag, D., Piccirilli, J. A., & Pyle, A. M. (1992) *J. Biol. Chem. 267*, 17479–17482.

Chamberlin, M. J., & Patterson, D. L. (1965) *J. Mol. Biol. 12*, 410–428.

Chou, S. H., Flynn, P., & Reid, B. (1989) *Biochemistry 28*, 2435–2443.

Davanloo, P., Rosenberg, A. H., Dunn, J. J., & Studier, F. W. (1984) *Proc. Natl. Acad. Sci. U.S.A. 81*, 2035–2039.

Davies, R. W., Waring, R. B., Ray, J. A., Brown, T. A., & Scazzacchio, C. (1982) *Nature 300*, 719–724.

Doudna, J. A., Cormack, B. P., & Szostak, J. W. (1989a) *Proc. Natl. Acad. Sci. U.S.A. 86*, 7402–7406.

Doudna, J. A., & Szostak, J. W. (1989b) *Nature 339*, 519–522.

Doudna, J. A., Couture, S., & Szostak, J. W. (1991) *Science 251*, 1605–1608.

Grosshans, C. A., & Cech, T. R. (1991) *Nucleic Acids Res. 19*, 3875–3880.

Guschlbauer, W., & Jankowski, K. (1980) *Nucleic Acids Res. 8*, 1421–1433.

Hall, K. B., & McLaughlin, L. W. (1991) *Biochemistry 30*, 10606–10613.

Herschlag, D. (1992) *Biochemistry 31*, 1386–1399.

Herschlag, D., & Cech, T. R. (1990a) *Biochemistry 29*, 10159–10171.

Herschlag, D., & Cech, T. R. (1990b) *Biochemistry 29*, 10172–10180.

Herschlag, D., & Cech, T. R. (1990c) *Nature 344*, 405–409.

Herschlag, D., Piccirilli, J. A., & Cech, T. R. (1991) *Biochemistry 30*, 4844–4854.

Herschlag, D., Eckstein, F., & Cech, T. R. (1993a) *Biochemistry 32*, 8299–8311.

Herschlag, D., Eckstein, F., & Cech, T. R. (1993b) *Biochemistry 32*, 8312–8321.

Inoue, T., & Cech, T. R. (1985a) *Proc. Natl. Acad. Sci. U.S.A. 82*, 648–652.

Inoue, T., Sullivan, F. X., & Cech, T. R. (1985b) *Cell 43*, 431–437.

Jaishree, T. N., van der Marel, G. A., van Boom, J. H., & Wang, A. H. J. (1993) *Biochemistry 32*, 4903–4911.

Katahira, M., Lee, S. J., Kobayashi, Y., Sutgeta, H., Kyogoku, Y., Iwai, S., Ohtsuka, E., Benevides, J. M., Thomas, G. J. (1990) *J. Am. Chem. Soc. 112*, 4508–4512.

Kunkel, T. A., Roberts, J. D., & Zakour, R. A. (1987) *Methods Enzymol. 154*, 367–382.

Lehman, I. R. (1974) *Science 186*, 790–797.

Lin, S. Y., & Riggs, A. D. (1972) *J. Mol. Biol. 72*, 671.

Martin, F. H., & Tinoco, I. (1980) *Nucleic Acids Res. 8*, 2295–2299.

Murphy, F. L., & Cech, T. R. (1989) *Proc. Natl. Acad. Sci. U.S.A. 86*, 9218–9222.

Michel, F., Hanna, M., Green, R., Bartel, D. P., & Szostak, J. W. (1989) *Nature 342*, 391–395.

Michel, F., & Westhof, E. (1990) *J. Mol. Biol. 216*, 585–610.

McConnell, T. S., Cech, T. R., & Herschlag, D. (1993) *Proc. Natl. Acad. Sci. U.S.A. 90*, 8362–8366.

Milligan, J. F., Groebe, D. R., Withereli, G. W., & Uhlenbeck, O. C. (1987) *Nucleic Acids Res. 15*, 8783–8798.

Moore, M. J., & Sharp, P. A. (1992) *Science 256*, 992–997.

Piccirilli, J. A., McConnell, T. S., Zaug, A. J., Noller, H. F., & Cech, T. R. (1992) *Science 256*, 1420–1424.

Pyle, A. M., McSwiggen, J. A., & Cech, T. R. (1990) *Proc. Natl. Acad. Sci. U.S.A. 87*, 8187–8191.

Pyle, A. M., & Cech, T. R. (1991) *Nature 350*, 628–631.

Pyle, A. M., Murphy, F. L., & Cech, T. R. (1992) *Nature 358*, 123–128.

Richards, E. G. (1975) in *Handbook of Biochemistry and Molecular Biology*: *Nucleic Acids* (Fasman, G. D., Ed.) 3rd ed., Vol. I, p 597, CRC Press, Cleveland, OH.

Riley, M., & Maling, B. (1966) *J. Mol. Biol. 20*, 359–389.

Salazar, M. Fedoroff, O. Y., Miller, J. M., Ribeiro, N. S., & Reid, B. R. (1993) *Biochemistry 32*, 4207–4215.

Sanger, F., Nicklen, S., & Coulson, A. R. (1977) *Proc. Natl. Acad. Sci. U.S.A. 74*, 5463–5467.

SantaLucia, J., Kierzek, R., & Turner, D. H. (1991) *J. Am. Chem. Soc. 113*, 4313–4322.

SantaLucia, J., Kierzek, R., & Turner, D. H. (1992) Science *256*, 217–219.

Sugimoto, N., Kierzek, R., & Turner, D. H. (1988) *Biochemistry 27*, 6384–6392.

Sugimoto, N., Sasaki, M., Kierzek, R., Bevilacqua, P. C., & Turner, D. H. (1989a) *Nucleic Acids Res. 17*, 355–371.

Sugimoto, N., Sasaki, M., Kierzek, R., & Turner, D. H. (1989b) *Chem. Lett. 12*, 2223–2226.

Sullivan, F. X., & Cech, T. R. (1985) *Cell 42*, 639–648.

Turner, D. H., Sugimoto, N., Kierzek, R., Dreiker, S. D. (1987) *J. Am. Chem. Soc. 109*, 3783–3785.

Uesugi, S., Miki, H., Ikehara, M., Iwahashi, H., & Kyogoku, Y. (1979) *Tetrahedron Lett. 42*, 4073–4076.

Walker, G. T. (1988) *Nucleic Acids Res. 16*, 3091–3099.

Wang, J. F., & Cech, T. R. (1992) *Science 256*, 526–529.

Wang, J. F., Downs, W. D., & Cech, T. R. (1993) *Science 260*, 504–508.

Waring, R. B., Towner, P., Minter, S. J., & Davies, R. W. (1986) *Nature 321*, 133–139.

Weeks, K. M., & Crothers, D. M. (1992) *Biochemistry 31*, 10281–10287.

Young, B., Herschlag, D., & Cech, T. R. (1991) *Cell 67*, 1007–1019.

Zaug, A. J., Kent, J. R., & Cech, T. R. (1984) *Science 224*, 574–578.

Zaug, A. J., Been, M. D., & Cech, T. R. (1986) *Nature 324*, 429–433.

Zaug, A. J., Grosshans, C. A., & Cech, T. R. (1988) *Biochemistry 27*, 8924–31.